Mineralogical changes and associated decrease in tritiated water diffusivity after alteration of cement–bentonite interfaces

TETSUJI YAMAGUCHI[1,*], TAKUMA SAWAGUCHI[1], MANABU TSUKADA[1], SEIICHI HOSHINO[2] AND TADAO TANAKA[1]

[1] *Nuclear Safety Research Center, Sector of Nuclear Safety Research and Emergency Preparedness, Japan Atomic Energy Agency, Tokai, Ibaraki 319-1195, Japan*
[2] *Central Research Laboratory, Taiheiyo Cement Corp., 2-4-2 Osaku, Sakura, Chiba 285-8655, Japan*

ABSTRACT: Alteration of cement–bentonite interfaces and accompanying changes in diffusivity of tritiated water (HTO) was investigated experimentally using intact, hardened cement-paste specimens. The alteration by carbonate solution was accompanied by mineralogical changes at the interface and a decrease in the HTO diffusivity to $\sim$70 ± 7% of the initial value after a 180-day period. Another alteration in contact with compacted bentonite was accompanied by mineralogical changes at the interface and a decrease in the HTO diffusivity to $\sim$71 ± 10% of the initial value after a 600-day period. The changes in the diffusivity were considerably less than those observed for mixed specimens of ground, granulated hardened cement paste and bentonite where the diffusivity decreased to 20% of the initial value over 180 days. The results were extrapolated to 15 y under simple assumptions and showed good agreement with those observed in the cement–argillite interface at Tournemire URL (France). Such an explanation enhances confidence in the assessment of the alteration of cement-bentonite systems and might be a basis for using the data and models obtained in the long-term assessment of radioactive waste disposal.

Highly alkaline groundwater induced by cementitious materials in a deep geological isolation system of high-level radioactive waste is likely to alter bentonite buffer materials and to deteriorate the physical and/or chemical barrier functions of the buffer materials. In order to evaluate the long-term alteration behavior, understanding of the phenomena occurring at the interface between bentonite and cementitious materials is essential, especially changes in transport properties through the interface accompanying mineralogical

alterations. Although the cement–clay interfacial reactions have been studied thoroughly (*e.g.* Fernández *et al.*, 2013; Bartier *et al.*, 2013), reliable evidence has not been given for the clogging of the pores due to the formation of secondary minerals. Hoshino *et al.* (2009) studied the diffusivity of tritiated water through mixed specimens of ground, granulated hardened cement paste and bentonite, and suggested that the diffusivity decreased with aging to 20% of the initial value over 180 days. The relationship between such significant change in diffusivity and those occurring at interfaces between bentonite and intact cementitious materials, however, has not been clarified. In the present study, alteration of

cement–bentonite interfaces and accompanying changes in diffusivity of tritiated water was investigated experimentally using intact hardened cement-paste specimens.

EXPERIMENTAL

Two types of experiments were performed. The first simulated alteration of hardened-cement paste with carbonate/bicarbonate anions supplied by bentonite (Fig. 1a). The carbonate anions were supplied from aqueous solution without using bentonite. The cement specimens were prepared from ordinary Portland cement (OPC) the chemical composition of which was shown elsewhere (Yamaguchi *et al.*, 2009). Hardened cement-paste specimens were prepared by mixing the OPC with deionized water at water:cement weight ratios (W/C) of 0.45, 0.6 and 0.75, placing in moulds and curing at 50°C in deionized water for 45 days until the XRD peaks for unhydrated cement had disappeared. The W/C ratios of 0.6 and 0.7 were

a
Hardened cement
30 mm in diameter, 10 mm thick

0.5 M Na_2CO_3 solution (110 cm³) with HTO

0.5 M Na_2CO_3 solution (110 cm³)

b
Hardened cement
30 mm in diameter, 5 mm thick

Compacted bentonite
30 mm in diameter, 5 mm thick

HTO was added into cement side in diffusion experiment.

Cement equilibrium solution (110 cm³)
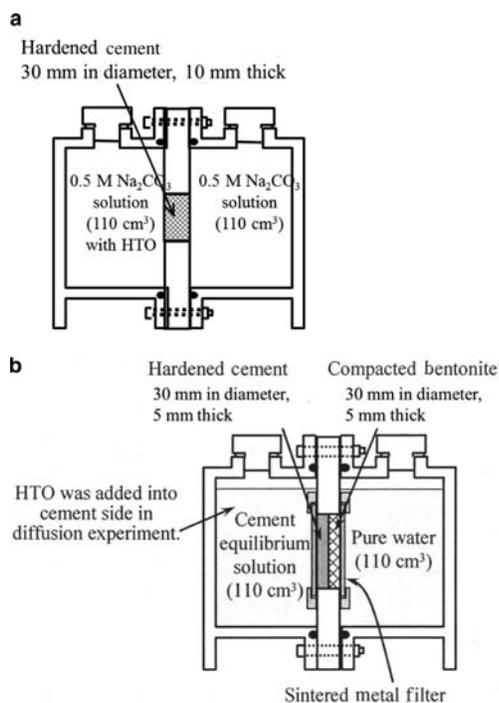
Pure water (110 cm³)

Sintered metal filter

Fig. 1. Experimental configuration of alteration and diffusion experiments for cement carbonation tests: (a) at room temperature and for cement–bentonite interface tests; (b) at 50°C during alteration and at room temperature during diffusion experiments for tritiated water.

selected to accelerate the alteration process and to observe the effects of the alteration in a reasonable time period. The curing temperature of 50°C was selected to accelerate complete hydration without causing changes in cement mineralogy. The cylindrical, hardened cement specimens, 30 mm in diameter and 10 mm thick, were fitted into the central part of an acrylic through-diffusion cell by dry abrasion with abrasive papers, and were vacuum dried. Each specimen was embedded in the through-diffusion cell (Fig. 1a) filling any gaps between the specimen and the acrylic wall with epoxy resin. After assembling the diffusion cell, the specimen was soaked in 1.5 M $NaClO_4$ solution at pH 11 under vacuum for 1 day to evacuate all air from the interconnected pores. The ionic strength and the pH were selected for preconditioning the specimen with the solution used in the subsequent cement carbonation test (0.5 M Na_2CO_3), and perchlorate was selected as a non-complexing anion. Through-diffusion of tritiated water was observed for 30 days at room temperature (25 ± 8°C) under $NaClO_4$ solution by adding tritiated water to one of the reservoirs to achieve a concentration of 1.0×10^2 Bq/cm^3. After the effective diffusion coefficient of tritium through the specimen was obtained according to Yamaguchi *et al.* (2009), the water was replaced by 0.5 M Na_2CO_3 solution with pH 11 and diffusion of tritium was observed by adding tritiated water to one of the reservoirs (1.0×10^3 Bq/cm^3). Mock-up specimens, multiple similar specimens without addition of tritiated water, were analysed by XRD, thermal analysis (TGA-DTA) and mercury intrusion porosimetry (MIP) after reaction with 0.5 M Na_2CO_3 solution with pH 11 for 3, 7, 15, 28, 91, 180 and 365 days.

The second type of experiment simulated the alteration of hardened cement paste in contact with compacted bentonite (Fig. 1b). The W/C ratio and the thickness of the hardened cement specimen were 0.6 and 5 mm, respectively. The Kunigel V1 bentonite was weighed and was set adjacent to the hardened cement paste specimen by a pressing machine to achieve a dry density for the bentonite of 1.6 g/cm^3. Cement-equilibrated water was prepared and placed in the cement-side reservoir which was filled with deionized water. The diffusion cell was kept under vacuum for 1 day to evacuate all air from the interconnected pores. The cement-bentonite specimens including mock-up specimens were allowed to react at 50°C for 0, 28, 91, 182, 300 and 600 days. The temperature elevated to 50°C is advantageous because the alteration at the cement–bentonite interface is expected to be more clearly detected by XRD; alteration of the hardened

cement paste alone can be ignored and the easy-to-use acrylic diffusion cell is durable. After the reaction periods, tritiated water was added to the cement-side reservoir (1.0×10^2 Bq/cm^3) to determine the diffusion coefficient of tritium through the cement–bentonite specimen at room temperature ($25 \pm 8°$C). The diffusion coefficient through the cement alone was also determined after removing the bentonite with a spatula. No effect of the removal of the bentonite on the tightness between the specimen and the wall was detected. Mock-up specimens were analysed by XRF, XRD, TGA-DTA, methylene-blue absorption titration, exchangeable cations determination and MIP. Chemical analysis by XRF conformed to JIS R 5204: 2002 (Japanese Standard Association, 2011).

Experiments were performed under inert atmosphere (argon). The hardened cement paste and the bentonite mock-up specimens were analysed after drying for 2 weeks under Ar at a relative humidity of 11%.

RESULTS

The first series of experiments (cement carbonation tests) showed dissolution of Ca(OH)$_2$ and ettringite and formation of calcite (Fig. 2). Calcite was formed at the interfaces between the cement and the Na$_2$CO$_3$ solution and at the interior of the cement specimen (Fig. 2), especially rapidly at the interface as shown in the TGA-DTA diagrams (Fig. 3). Decrease in the pore diameters and the slight decrease in the porosity at the interfaces were observed by MIP.

Figure 4a shows the concentration of tritium with time both in high-concentration and low-concentration reservoirs. The concentrations of tritium in the high-concentration reservoirs decrease and those in the low-concentration reservoirs increase with time. As discussed by Yamaguchi *et al.* (2009), when the increasing rates are identical to the decreasing rates, the steady state flux of tritiated water is established in the cylindrical, hardened cement paste. The effective diffusivity was evaluated using equation 1 based on Fick's law:

$$J = -D_e \partial c / \partial x \qquad (1)$$

where J is the diffusive flux (Bq/m^2/s) D_e is the effective diffusivity, and $\partial c / \partial x$ is the concentration gradient (Bq/m^4). The diffusive flux was obtained from:

$$J = (\Delta c_2 / \Delta t) V A^{-1} \qquad (2)$$

where $\Delta c_2 / \Delta t$ is the rate of increase of the concentration of tritium (Bq/m^3/s), V the volume of the solution in the reservoir (1.1×10^{-4} m^3) and A is the cross section of the hardened cement-paste specimen (7.065×10^{-4} m^2). The value of $\Delta c_2 / \Delta t$ was obtained from the slope of the linear approximation of the through-diffusion curves. The concentration gradient, $\partial c / \partial x$, was obtained from a difference in the concentrations of tritium in the two reservoirs as:

$$\partial c / \partial x = (\overline{c_1} - \overline{c_2}) L_T^{-1} \qquad (3)$$

where L_T is the thickness of the specimens (0.01 m), $\overline{c_1}$ is the average concentration of tritium in the high-concentration reservoir (Bq/m^3) and $\overline{c_2}$ is the average concentration of tritiated water in the low-concentration reservoir (Bq/m^3). Effective diffusivities were obtained by combining equations 1, 2 and 3.

In analysing the data shown in Fig. 4a, the effective diffusivity of the tritium through the hardened cement-paste specimen at each time was evaluated by analysing 15 concentration data points before and after the time (preceding seven data points, one data point at the time and the following seven data points) using equations 1–3 (Fig. 4b). The 15 concentration data points were necessary to obtain $\Delta c_2 / \Delta t$ with reasonably small uncertainties (~2% in 2σ). At the beginning of the carbonation tests, the effective diffusivity was not determined because the increasing rates of the tritium concentration in the low-concentration reservoir were not identical to the decreasing rates of the tritium concentration in the high-concentration reservoir, namely, the steady-state flux of tritiated water was not established. The effective diffusivities obtained here are overall effective diffusivities through partially altered specimens as is discussed below.

The effective diffusivity of tritium decreased with time from $(5.0 \pm 0.4) \times 10^{-11}$ m^2/s to $(3.5 \pm 0.3) \times 10^{-11}$ m^2/s for W/C of 0.6 (Fig. 4b). The effective diffusivity decreased by 70 ± 7% of the initial value after 180 days. Uncertainties (2σ) of the diffusivity propagated from the uncertainties in sizes of the specimen (5–10%), concentration measurements (2%) and data fitting (2–5%) were shown. No significant change in diffusivity was observed for W/C of 0.45 although a variation of $\pm$ 20% was observed. The diffusivity was halved over 150 days for W/C of 0.75. Considering the fact that the effective diffusivity for W/C of 0.45 varies between 1.6×10^{-11} m^2/s and 2.8×10^{-11} m^2/s, the possibility that the decrease in the diffusivity for W/C of 0.6 to 70% is within the range of variation or a result of modelling artifact cannot be discounted. Further study is necessary to demonstrate the
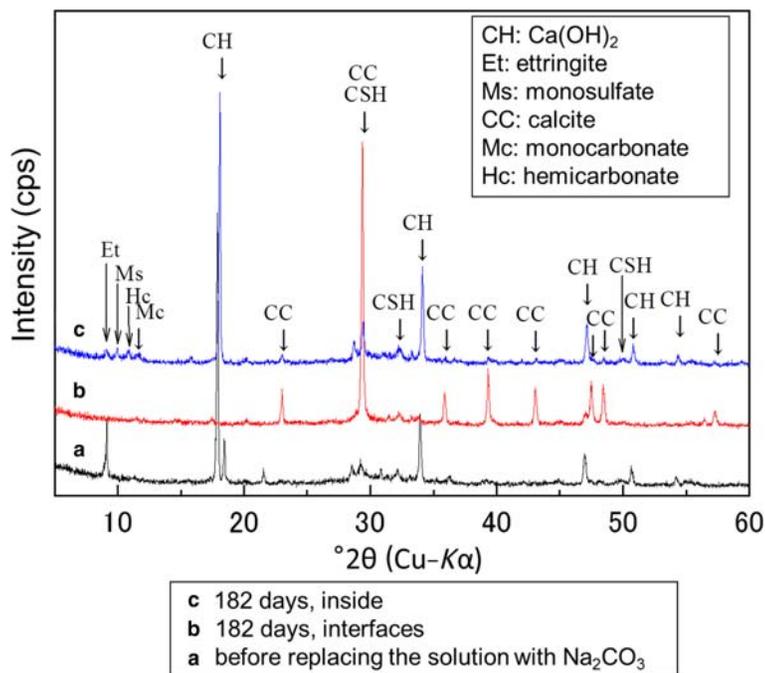
FIG. 2. XRD patterns of hardened cement-paste specimens (experiment 1): (a) original cement paste before replacing the NaClO$_4$ solution with Na$_2$CO$_3$; (b) interface between the cement and the Na$_2$CO$_3$ solution for 182 days; and (c) interior of the cement specimen.

accuracy and reliability of the modelling of the simultaneous alteration and diffusion experiments and to reduce accompanying uncertainties.

The second experiment for the cement–bentonite interface showed dissolution of Ca(OH)$_2$ and the formation of calcite and katoite in the cement
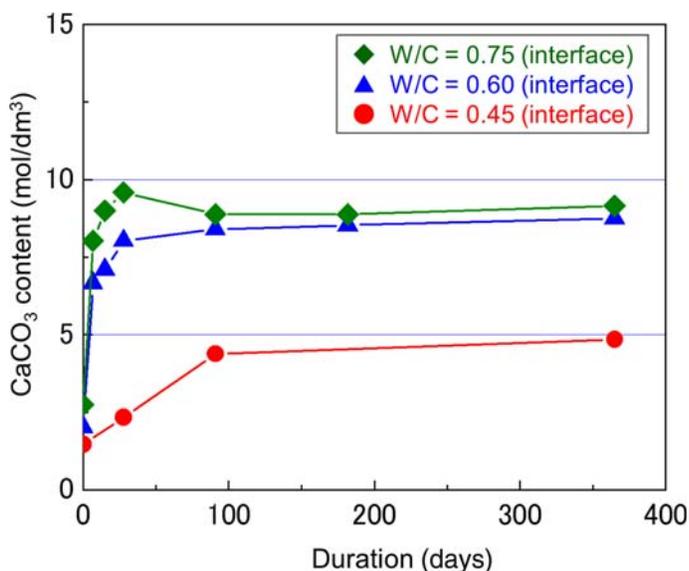
FIG. 3. Increase in the amount of CaCO$_3$ per dm^3 with duration of alteration determined by TGA-DTA.
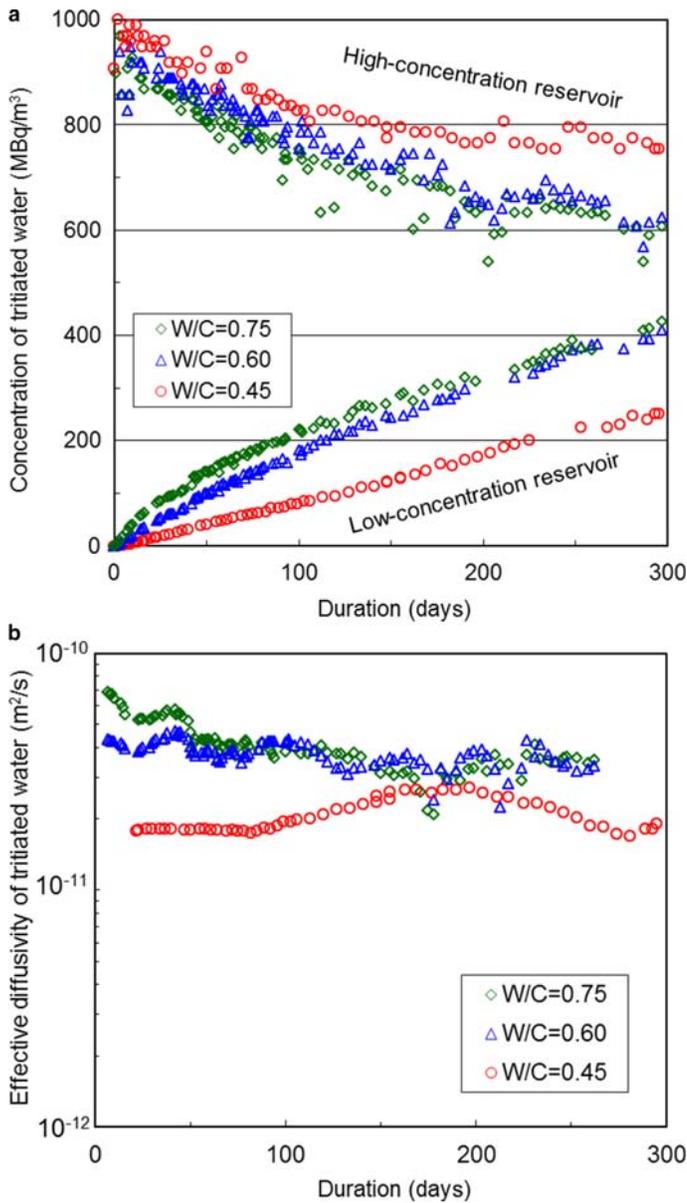
FIG. 4. (a) Changes in the concentration of tritiated water in the two reservoirs; (b) evaluated effective diffusivity through the hardened cement-paste specimens.

(Fig. 5a). Mineralogical changes were not clearly visible in the bentonite (Fig. 5b). The results of the chemical analysis of the cement and the bentonite showed that calcium migrated from cement to bentonite whereas Si, Al, Mg and S migrated from bentonite to cement. Exchangeable Ca^{2+} of the bentonite increased from 10% of CEC to 90%. According to the TGA-DTA results the

amount of calcite decreases in bentonite and increases in cement. The MIP results showed that the porosity of hardened cement paste increased from 37% to 40% (W/C = 0.6) and the pores of <0.01 μm in diameter increased with alteration progress.

The effective diffusivity through the overall cement and bentonite decreased from $(7.4 \pm 0.8) \times 10^{-11}$ m^2/s to
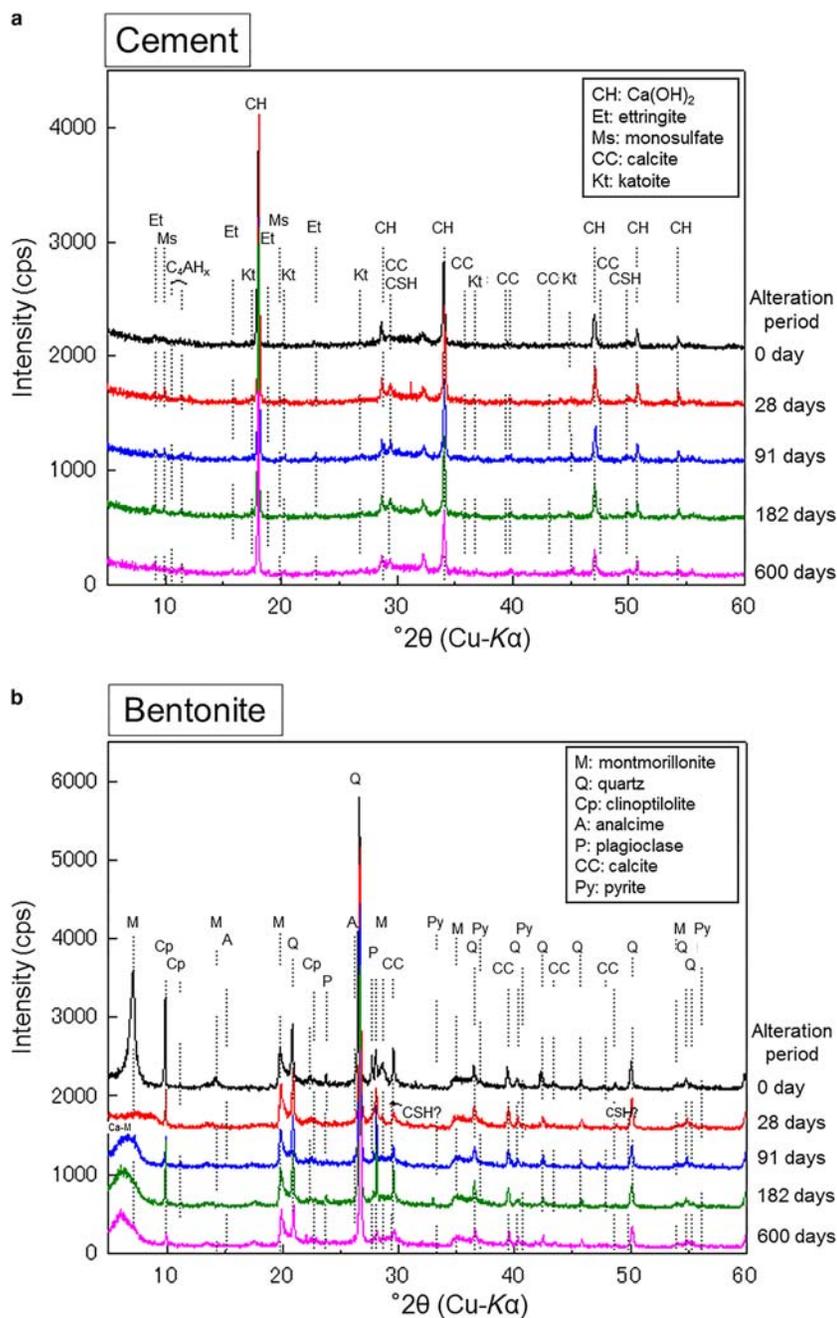
FIG. 5. XRD patterns of hardened cement and bentonite subject to alteration for 0–600 days of reaction (experiment 2).

$(5.1 \pm 0.5) \times 10^{-11}$ m²/s during the 600 days (W/C = 0.6) (Fig. 6). The decrease was caused by the decrease in the diffusivity in the hardened cement paste from $(4.2 \pm 0.4) \times 10^{-11}$ m²/s to $(3.0 \pm 0.3) \times 10^{-11}$ m²/s (Fig. 6).

The effective diffusivity decreased to $71 \pm 10\%$ of the initial value after 600 days. The reason for the decrease in the diffusivity observed in the present two types of experiments should be the same as that in the
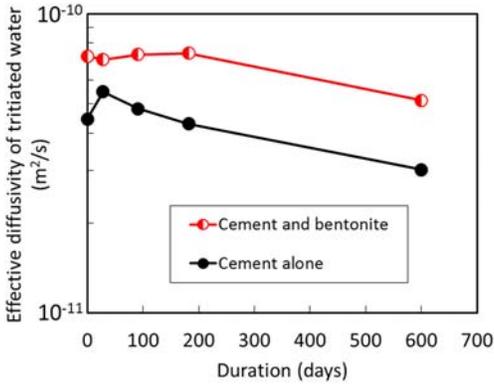
FIG. 6. Changes in effective diffusivity of tritiated water through cement–bentonite and for cement alone throughout the alteration.

experiments for mixed specimens of ground, granulated, hardened cement paste and bentonite (Hoshino *et al.*, 2009), because the mineralogical modifications observed (dissolution of $Ca(OH)_2$ and formation of calcite and katoite in hardened cement paste) were common to all the experiments.

DISCUSSION

The changes in the diffusivity were smaller than those observed by Hoshino *et al.* (2009). Alteration of interfaces was more intense in the experiments using ground, granulated, hardened cement paste (Hoshino *et al.*, 2009) than the present experiments. The difference can be explained by the presence of different reactive surface areas: 14.13 cm^2 for the cement carbonation tests, 7.07 cm^2 for the cement–bentonite interface tests and 104 cm^2 for the experiment using ground, granulated hardened cement paste (Hoshino *et al.*, 2009). The depth of mineralogical alteration and changes in diffusivity were limited at the interface in the present experiments. Assuming that the decrease in diffusivity occurs at limited alteration depths at the interfaces, the equivalent diffusivity ($D_{e,equiv}$) of the specimens can be evaluated as:

$$1/D_{e,equiv} = x/D_{e,alt} + (1-x)/D_{e,0} \qquad (4)$$

where $D_{e,alt}$ is the decreased diffusivity of alteration depth (m^2/s), $D_{e,0}$ is the initial diffusivity (m^2/s) and x is the ratio of the depth of alteration to the total thickness. Equation 4 is derived by applying Fick's law to the steady-state diffusion through the partially

altered system shown in Fig. 7 as:

$$J = D_{e,equiv}\Delta c/L = D_{e,0}\Delta c_0/L(1-x)$$
$$= D_{e,alt}\Delta c_{alt}/Lx \qquad (5)$$

where Δc is equal to a sum of Δc_{alt} and Δc_0.

Because the diffusivity can be assumed to decrease to 20% of the initial value in the experiments in which ground, granulated hardened cement paste and bentonite reacted thoroughly (Hoshino *et al.*, 2009), $D_{e,alt}$ was replaced by $0.2 D_{e,0}$ and equation 4 was simplified as:

$$D_{e,equiv}/D_{e,0} = 1/(4x+1). \qquad (6)$$

This equation gives an x value of 0.11 ± 0.04 for the cement carbonation tests, which means that the depth of alteration is 1.1 ± 0.4 mm for two reactive surfaces, *i.e.* 0.55 ± 0.20 mm for each surface for 180 days. The x value of 0.10 ± 0.05 was estimated for the cement–bentonite interface tests, which means a 0.5 ± 0.3 mm depth was altered over 600 days.

The depth of alteration, L (mm), would be proportional to the square root of time because the alteration is driven by the diffusive transport of solute:

$$L = a\sqrt{t} \qquad (7)$$

where a is a proportional constant (mm y$^{-0.5}$) and t is the duration of alteration (y). The proportional constant was determined for the cement carbonation and cement–bentonite interface tests (Table 1).

The depths of alteration over 15 y were estimated to be 3.0 ± 1.0 mm for the cement carbonation tests and 1.5 ± 0.8 mm for the cement–bentonite interface tests by using the a values of Table 1. Mineralogical characterization of a concrete–argillite interface that experienced 15 y of interaction at Tournemire URL, France (Tinseau *et al.*, 2006; De Windt *et al.*, 2008; Gaboreau *et al.*, 2011) indicated the formation of calcite and changes in grain densities within the first centimetre (Tinseau *et al.*, 2006; Gaboreau *et al.*, 2011). On the other hand, dissolution of quartz and the formation of C-S-H was observed only in the first millimetres of the interface (Tinseau *et al.*, 2006; De Windt *et al.*, 2008). The depths of alteration for cement carbonation and cement–bentonite interface tests estimated in this study are in agreement with those observed at the cement–argillite interface at Tournemire URL (France).

The discussion here is based on results from experiments using hardened cement paste with a W/C ratio of 0.6 (a very high value not to be exceeded in concrete technology). A positive correlation is
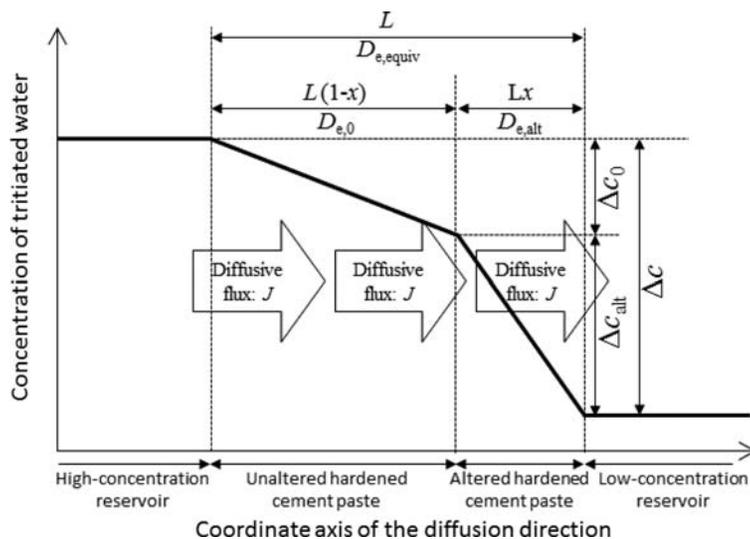
FIG. 7. Schematic view of steady-state diffusion of tritiated water through a partially altered hardened cement-paste specimen.

TABLE 1. The depth of alteration, L, and the proportional constant, a, estimated for the experiments for cement carbonation and cement–bentonite interface tests.

Parameter	Cement carbonation tests	Cement–bentonite interface tests
t (y)	0.492	1.643
L (mm)	0.55 ± 0.20	0.50 ± 0.26
a (mm y$^{-0.5}$)	0.76 ± 0.26	0.39 ± 0.20

inferred between the degree of alteration and the W/C ratio (Figs 3, 4).

CONCLUSIONS

Laboratory experiments revealed the mineralogical changes at cement–bentonite interfaces and accompanying changes in the diffusivity of solute. A consistent explanation was given to the results from the alteration experiment using bentonite and ground, granulated, hardened cement paste (Hoshino *et al.*, 2009), the alteration experiment of hardened cement paste with carbonate/bicarbonate anions, the alteration experiment of bentonite and hardened cement paste and observation of cement–argillite interactions over 15 y at the Tournemire URL (France). Such an explanation enhances our confidence in the assessment of the

alteration of cement–bentonite systems and might be a basis for using the data and models in the present study in long-term assessment of radioactive waste disposal. The modelling procedure for the simultaneous alteration and diffusion experiments needs to be verified in the future.

REFERENCES

Bartier D., Techer I., Dauzeres A., Boulvais P., Blanc-Valleron M.-M. & Cabrera J. (2013) *In situ* investigation and reactive transport modelling of cement paste/argillite interactions in a saturated context and outside an excavated disturbed zone. *Applied Geochemistry*, **31**, 94–108.

De Windt L., Marsal F., Tinseau E. & Pellegrini D. (2008) Reactive transport modeling of geochemical interactions at a concrete/argillites interface, Tournemire site (France). *Physics and Chemistry of the Earth*, **33**, S295–S305.

Fernández R., de la Villa R.V., Ruiz A.I., Garcia R. & Cuevas J. (2013) Precipitation of chlorite-like structures during OPC porewater diffusion through compacted bentonite at 90°C. *Applied Clay Science*, **83–84**, 357–367.

Gaboreau S., Prêt D., Tinseau E., Claret F., Pellegrini D. & Stammose D. (2011) 15 years of *in situ* cement-argillite interaction from Tournemire URL: Characterization of the multi-scale spatial heterogeneities of pore space evolution. *Applied Geochemistry*, **26**, 2159–2171.

Hoshino S., Yamaguchi T., Maeda T., Mukai M., Tanaka T. & Nakayama S. (2009) Mineralogical changes of cement and bentonite accompanied with their interactions. Pp. 445–452 in: *Scientific Basis for Nuclear Waste Management*, XXXIII (B.E. Burakov & A.S. Aloy, editors). Cambridge University Press, UK.

Japanese Standard Association (2011) Chemical analysis method of cement by X-ray fluorescence, JIS R 5204: 2002. Pp. 893–903 in: *JIS Handbook 10*, Ready-mixed Concrete – 2011. Japanese Standard Association, Tokyo (in Japanese).

Tinseau E., Bartier D., Hassouta L., Devol-Brown I. & Stammose D. (2006) Mineralogical characterization of the Tournemire argillite after in situ interaction with concretes. *Waste Management*, **26**, 789–800.

Yamaguchi T., Negishi K., Hoshino S. & Tanaka T. (2009) Modeling of diffusive mass transport in micropores in cement based materials. *Cement and Concrete Research*, **39**, 1149–1155.